ISBN: 978-3-95450-238-7 ISSN: 2226-0358 doi:10.18429/JACoW-ICALEPCS2023-TUMBCM034

MOTION CONTROL ARCHITECTURE AND KINEMATICS FOR MULTI-DOF KIRK-PATRICK-BAEZ FOCUSING MIRRORS SYSTEM AT LNLS-SIRIUS *

J. P. S. Furtado†, J. V. E. Matoso, T. R. S. Soares, G. B. Z. L. Moreno, C. S. C. Bueno,
M. A. B. Montevechi Filho, Brazilian Synchrotron Light Laboratory, CNPEM, Campinas, Brazil

Abstract

In modern 4th generation synchrotron facilities, piezo actuators are widely applied due to their nanometric precision in linear motion and stability. This work shows the implementation of a switching control architecture and a tripod kinematics for a set of 4 piezo actuators, responsible by positioning a short-stroke, the vertical and horizontal focusing mirrors of the Kirkpatrick-Baez mirror system at MOGNO Beamline (X-Ray Microtomography). The switching control architecture was chosen to balance timing to move through the working range (changing the beam incidence on stripes of low/high energy), resolution and infrastructure costs. This paper also shows the implementation and results of the layered kinematics, developed to uncouple short-stroke from long-stroke to fix any parasitic displacements that occur on the granite bench levellers due to motion uncertainty and mechanism non-linearities, and to match the required beam stability without losing alignment flexibility or adjustment repeatability. The architecture was built between a PIMikroMove set of driver-actuators and an Omron Delta Tau Power Brick LV controller due to its standardization across the control systems solutions at Sirius, ease of control software scalability and its capability to perform calculations and signal switching for control in C language, with real-time performance to make adjustments to the angles responsible by focusing the beam in a speed that matches the required position stability, guaranteeing the necessary resolution for the experiments.

INTRODUCTION

A new version of the Kirkpatrick-Baez focusing mirror system has been designed and installed in the MOGNO Beamline [1] (X-Ray Microtomography) at the Brazilian Synchrotron Light Laboratory [2] (LNLS), with extra features and implementations in comparison with other focusing systems currently working in other beamlines operation, in addition with smaller stability requirements — 8 nrad (RMS) for the horizontal focusing mirror (HFM) pitch angle, and 50 nrad for the pitch angle and 10 nm (RMS) for the translation of the vertical focusing mirror (VFM), in which both of them belong to the short-stroke subsystem, operating in high vacuum [3] (between 10^{-9} mbar and 10^{-9} mbar). The system implementation features a long-stroke, represented by a granite bench [4], which main function is to select the specific stripe for the experiment – low or high energy, present in both mirrors –, but also to filter noises provided by floor vibrations and other scientific equipment. To accomplish with this functionality, the system was designed in order to implement a kinematics by layers. By doing this, there are two acting kinematic subsystems that, together, represent a numerical construction that allows a stripe selection in both horizontal and vertical focusing mirrors by moving both strokes in a determined cartesian direction – and that's what makes this implementation ubiquitous and innovative in the new Brazilian Synchrotron Light Source, as the reported results in terms of flexibility, stability and repeatability have become essential and unprecedent for the experiments in the beamline.

KINEMATICS BY LAYERS

As mentioned before, the kinematic motion in a layered structure has been designed in order to provide a high resolution motion capacity for adjustment, and reasonable time for changing stripes – between high and low energies – in the same mechanism by moving the strokes in a single cartesian direction. Figure 1 shows the internal mechanism during its commission-ing while the vacuum chamber was opened in a clean room (following the ISO 6 norm), responsible by focusing the synchrotron beam across the Z direction, following the laboratory convention guidelines [5]. The two stripes of the HFM are distributed in the Y direction, in which each center is separated in 7 mm – and that also happens with the vertical focusing mirror, but in the X direction.

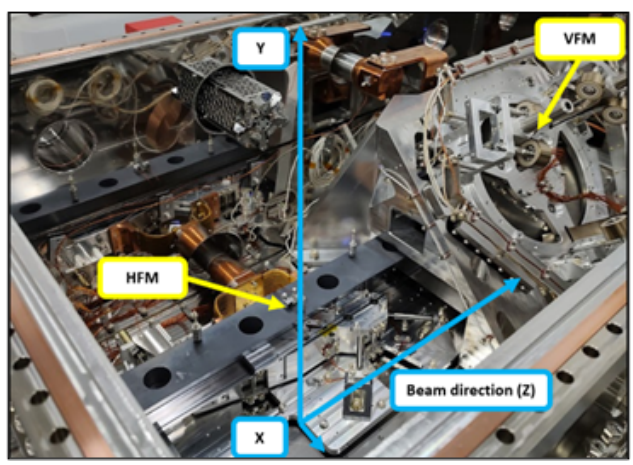

Figure 1: Internal mechanism containing vertical and horizontal focusing mirrors during the commissioning of the short-stroke.

Figure 2 shows the assembly between the long-stroke –

* Work supported by the Ministry of Science, Technology and Innovation.
† joao.furtado@lnls.br

ISBN: 978-3-95450-238-7 ISSN: 2226-0358 doi:10.18429/JACoW-ICALEPCS2023-TUMBCM034

represented by the bench containing the granites – and the short-stroke – represented by the vessel, positioned on the top granite. Since the short stroke of the HFM has only one degree of freedom (fine rotation of Ry provided by a piezo actuator), the top granite is responsible for translating in the Y direction, using a set of three levelers in a tripod configuration [5] – in order to select the stripe to accept the beam: 3.5 mm to select the low-energy stripe, and −3.5 mm for high-energy. In the other hand, a set of three piezoelectric actuators positioned as a tripod (such as the levelers) control the pitch angle (Rx), the roll angle (Rz) and a translation in an orthogonal axis that is aligned with a diagonal direction between Y and X directions – equally distant in 45 degrees between each cartesian axis –, as the normal vector of the plane composed by this tripod is parallel to this specific direction. So, to select the stripe in the vertical focusing mirror, the motion in this direction is necessary. The movement in this mirror, provided by the piezoelectric actuators, fixes its position in the Y direction after the selection provided by the granite bench and also selects the specific stripe of the vertical focusing mirror – note a commanded position equal to 3.5 mm in the Y cartesian direction is accompanied by a 3.5 mm in the X cartesian direction (in the laboratory convention, explicit in Figs. 1 and 2).

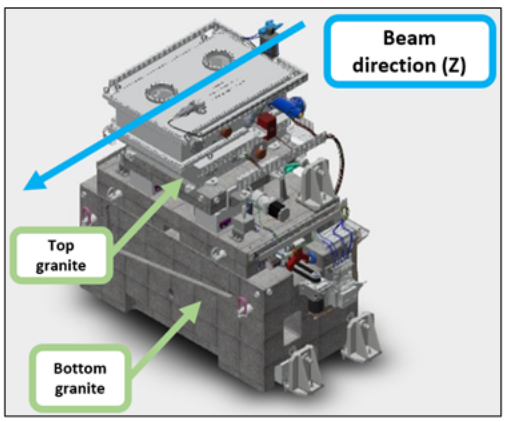

Figure 2: Assembly drawing containing granites and the vacuum vessel (where the internal mechanism is assembled).

FORWARD KINEMATICS

Modelling

As mentioned in the last sections, the set of three piezoelectric actuators that control the fine adjustment of the vertical focusing mirror is contained in a tripod construction, and that's a exactly-determined system that can be interpreted as a 3x3 robot [6], in which the controlled degrees of freedom are the position in Y cartesian direction – which is perfectly reflected in the X cartesian direction, following the project design tolerances –, and the pitch/roll orientations. The plane composed by the piezoelectric actuators – which is rotated in 45 degrees in the laboratory Z axis, as mentioned before – has its own reference, and they will be called $T_{y'}$ (position), $\theta_{x'}$ (pitch) and $\theta_{z'}$ (roll).

The piezoelectric actuators are the N-470-22UY stages, manufactured by PIMikroMove [7], and the feedback is reported by a set of three RL26BVS001C30V1 encoders (1 nm of resolution, absolute feedback, 26 bits [8]). The connections and closed loop control will be explained posteriorly, in this work. The encoders, to accomplish with the kinematic solving and to build a solvable numerical system, were assembled in parallel with the actuators, so the feedback contains the position aligned with the plane composed by the tripod of stages – with the crescent scale aligned with Y' axis. Figure 3 shows the tripod in the plane of the stages, aligned with the orthogonal axis between axes X and Y of the laboratory – in this orientation convention, the roll angle is aligned Z' axis, pitch angle is aligned with X' axis and the cartesian position is aligned with Y' axis.

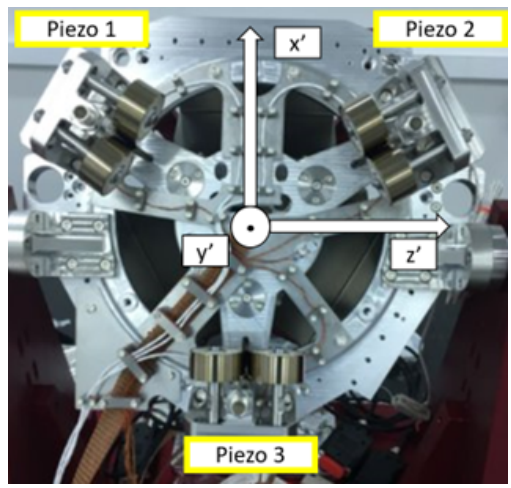

Figure 3: Mechanism of the vertical focusing mirror with orthogonal composition of axis that are aligned with the controlled degrees of freedom.

The mechanism also has a set of three constant-force springs, responsible by preloading and retracting the whole mechanism after being pushed by the stages and accomplishing with the tight tolerances of the chosen materials. Having this on mind is essential to fully understand the *Control Architecture* section, in which the motion control will be explained and demonstrated.

As the encoders measure pure positions in nanometers and the orientations are desired, then some equations must be solved in order to obtain the corresponding values of the controlled degrees of freedom. The encoders readings $p_i, i \in [1, 2, 3]$, in function of $T_{y'}$, $\theta_{x'}$ and $\theta_{z'}$, are the following ones:

$$p_1 = \begin{bmatrix} 0 & 1 & 0 \end{bmatrix} \cdot \left(Rot_x(\theta_{x'}) \cdot Rot_z(\theta_{z'}) \cdot \begin{bmatrix} r_{1,x'} \\ r_{1,y'} \\ r_{1,z'} \end{bmatrix} + \begin{bmatrix} 0 \\ T_{y'} \\ 0 \end{bmatrix} \right) \quad (1)$$

ISBN: 978-3-95450-238-7 ISSN: 2226-0358 doi:10.18429/JACoW-ICALEPCS2023-TUMBCM034

$$p_2 = \begin{bmatrix}0 & 1 & 0\end{bmatrix} \cdot \left(Rot_x(\theta_{x'}) \cdot Rot_z(\theta_{z'}) \cdot \begin{bmatrix} r_{2,x'} \\ r_{2,y'} \\ r_{2,z'} \end{bmatrix} + \begin{bmatrix} 0 \\ T_{y'} \\ 0 \end{bmatrix} \right) \quad (2)$$

$$p_3 = \begin{bmatrix}0 & 1 & 0\end{bmatrix} \cdot \left(Rot_x(\theta_{x'}) \cdot Rot_z(\theta_{z'}) \cdot \begin{bmatrix} r_{3,x'} \\ r_{3,y'} \\ r_{3,z'} \end{bmatrix} + \begin{bmatrix} 0 \\ T_{y'} \\ 0 \end{bmatrix} \right) \quad (3)$$

In which $r_{i,\gamma}$, $\gamma \in [x', y', z']$ $i \in [1, 2, 3]$, are the positions of the encoders in the plane composed by X' and Z' axes – determined by the project design under specific tolerances between each subsystem. In this system, the dimensions are shown in Table 1.

Table 1: Position of Each Stage of the Vertical Focusing Mirror in the X'Y'Z' Space, in mm

$r_{i,\gamma}$	x'	y'	z'
1	$147 \cdot cos(\pi/3)$	0	$-147 \cdot sin(\pi/3)$
2	$147 \cdot cos(\pi/3)$	0	$147 \cdot sin(\pi/3)$
3	-147	0	0

In the other hand, the homogeneous transformations that represents rotations [9], as functions of a determined angular input α, are:

$$Rot_x(\alpha) = \begin{bmatrix} 1 & 0 & 0 \\ 0 & cos(\alpha) & sin(\alpha) \\ 0 & -sin(\alpha) & cos(\alpha) \end{bmatrix} \quad (4)$$

$$Rot_z(\alpha) = \begin{bmatrix} cos(\alpha) & -sin(\alpha) & 0 \\ sin(\alpha) & cos(\alpha) & 0 \\ 0 & 0 & 1 \end{bmatrix} \quad (5)$$

In order to obtain the current $T_{y'}$, $\theta_{x'}$ and $\theta_{z'}$ according to the feedback received from the encoders, a numerical method is necessary, as the relations are non-linear and hard to be solved analytically.

Numerical Solving

The numerical method used to solve the Forward Kinematics of this project is based on Newton-Raphson iterations [10]. The main objective here is to minimize the error e_i, in the i-th iteration. The general formula for the i-th iteration is the following one:

$$e_{i+1} = e_i + J^{-1}(e_i) G(p_{raw}, e_i) \quad (6)$$

In which e_i is the value of the results $T_{y',i}$, $\theta_{x',i}$ and $\theta_{z',i}$ to be numerically calculated in the i-th iteration:

$$e_i = \begin{bmatrix} T_{y',i} \\ \theta_{x',i} \\ \theta_{z',i} \end{bmatrix} \quad (7)$$

Also, J is the Jacobian matrix. It is based on partial derivatives of the forward kinematics relations, and its arguments are the values of the actual iteration e_i.

$$J(e_i) = \begin{bmatrix} \frac{\partial p_1}{\partial T_{y'}}(e_i) & \frac{\partial p_1}{\partial \theta_{x'}}(e_i) & \frac{\partial p_1}{\partial \theta_{z'}}(e_i) \\ \frac{\partial p_2}{\partial T_{y'}}(e_i) & \frac{\partial p_2}{\partial \theta_{x'}}(e_i) & \frac{\partial p_2}{\partial \theta_{z'}}(e_i) \\ \frac{\partial p_3}{\partial T_{y'}}(e_i) & \frac{\partial p_3}{\partial \theta_{x'}}(e_i) & \frac{\partial p_3}{\partial \theta_{z'}}(e_i) \end{bmatrix} \quad (8)$$

Also, the G matrix is the minimization target, represented by the following expression:

$$G(p_{1,raw}, p_{2,raw}, p_{3,raw}) = \begin{bmatrix} p_{1,raw} - p_1(e_i) \\ p_{2,raw} - p_2(e_i) \\ p_{3,raw} - p_3(e_i) \end{bmatrix} \quad (9)$$

It is possible to realize that the G matrix receives the raw data read from encoders – represented by $p_{i,raw}$, $i \in [1, 2, 3]$, – and also the forward kinematics equations.

The Power Brick LV (PBLV) controller is the main computer in this system, which is used both for the calculations of the kinematic equations and for closing the control loop for all the axes of the mechanism. The PBLV takes an average of 430 microseconds to calculate the forward kinematics and 4 iterations of Newton's method, starting with zero initial values for each kinematics calculation:

$$e_0 = \begin{bmatrix} 0 \\ 0 \\ 0 \end{bmatrix} \quad (10)$$

To implement this formulation, the equations can be written and modelled using a Jupyter code – essentially in Python language –, as it performs matrix inversions, partial derivatives and expressions printing in C code using simple commands [11, 12]. Then the final equations – in C format – can be embedded into a real-time code in the PBLV, as it is capable of compiling and making executable files from C codes [13], increasing its applicability in solutions of precision engineering and mechatronic problems.

This is essential for the stability verification and positioning report to the experiment or to other scientific equipment based on triggering and synchronism, as the PBLV has a lot of functionalities when communicating with other high-level architectures, such as EPICS. Also, the calculation can be done without losing numerical precision, as the values running in C code – in long format – do not overflow. The main advantages are the fast conversion into the final values and possibility to implement in a real-time procedure, while the disadvantage is that this method only works for small angles – in the order of milliradians – which is compatible with the mechanism range. For higher angles, the calc values would not correspond to the reality of the feedback system.

CONTROL ARCHITECTURE

The control architecture is based on a low-level communication between the PBLV controller (which also controls the bench), especially its real-time code and the GPIO

ISBN: 978-3-95450-238-7 ISSN: 2226-0358 doi:10.18429/JACoW-ICALEPCS2023-TUMBCM034

board [13], and a PI E-872 driver to command the stages of the internal mechanism (vertical and horizontal focusing mirrors) by receiving the digital signals from the PBLV. For the internal mechanism – the objective of this section, as the control architecture for the bench is default and described in [5] –, the received setpoints from EPICS are the desired degrees of freedom $T_{y'}$, $\theta_{x'}$, $\theta_{z'}$, θ_y – the last one is the degree of freedom related to the horizontal focusing mirror, which does not have a complicated kinematics, as the mechanism is a rotating arm –, and the controller must apply the relations of the forward kinematics to find the desired final positions of each stage, as the closed-loop is based on the encoder reading.

The diagram shown in Fig. 3 implements the control architecture for both horizontal and vertical focusing mirrors of the internal mechanism. The C code runs in 1kHz switching frequency – it has been verified that this frequency does not bring real-time errors, making the control system deterministic –, and at every iteration of the loop it analyses one channel, in which:

- Channel 1 represents stage 1 of VFM;
- Channel 2 represents stage 2 of VFM;
- Channel 3 represents stage 3 of VFM;
- Channel 4 represents the stage of HFM.

The channel manager only goes to the next channel if the actual encoder being analyzed is inside a specific dead band. For this specific project, a dead band equal to 30 nm and SI-30nm has been found as enough to stabilize the system in a specific position.

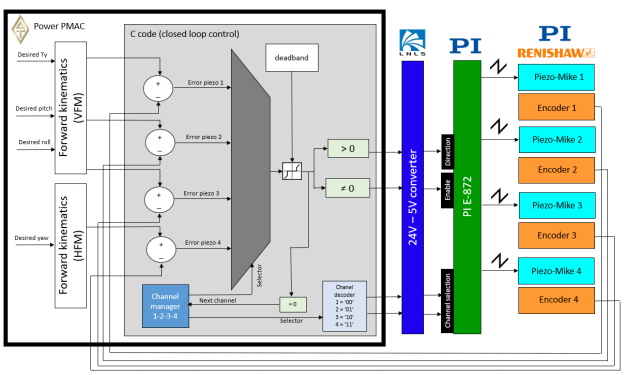

Figure 4: General control architecture in low-level between hardware, actuators and sensors.

The 24 V–5 V converter was manufactured by the electronic instrumentation group of LNLS, and the PIMikroMove driver is the E-872. The principal signals received by the driver are the direction, enable and the channel selector. The enable bit, when high, makes the driver produce several sawtooth waves in voltage, bringing motion to the stages. The switching frequency of the E-872 driver is configurable and was set up to 200 Hz, as it must be lower than the closed-loop control running inside the PBLV controller. High-er frequencies can be achieved in the sawtooth wave driver producer, but it was realized that it cannot pass 50 % of the closed-loop frequency, or the stage will not stop inside the dead band on time and will not stabilize following the beamline specifications by violating the RMS error requirements. Also, the multiplexer implemented inside the real-time code is necessary because the E-872 driver commands only one stage at a time, requiring some extra safety features whose will be explained later. The control architecture design for the piezoelectric actuators has demonstrated to be capable of bringing good performance in terms of movements repeatability, as this kind of actuators are widely applied in precision engineering due to their nano precision.

SAFETY IMPLEMENTATION

As mentioned before, some safety features had to be implemented in order to preserve the integrity of the internal mechanism, especially the vertical focusing mirror. To match that, some native implementations were integrated to the mechatronic control loop shown in the Fig. 4, such as the virtual motors as an abstraction for the set of stage-encoder. The virtual motors receive the set-point – it can come from the controller development environment or from EPICS – and have their feedback readings from the associated encoders. By having set-points and feedbacks, these virtual motors have associated following errors – these values feed the multiplexer shown in the Fig. 5, necessary for the low level closed-loop between the PBLV controller and the E-872 driver. The following errors feed the native safety manager – running inside the controller FPGA – and, according to their absolute values, an error flag that disables these virtual motors can be raised. This error flag is invisible to the E-872 driver, and when an error happens, all stages must be disabled to preserve the system integrity.

To mix the native implementations that brings safety due to the fast FPGA inside the controller with the personalized ones to accomplish with the project necessities, the scheme present in the Fig. 5 was developed. In this scheme, the Motor 0 – which is a virtual motor – is responsible by selecting which error will feed the closed-loop architecture in the real-time code – if the error is null, then the PBLV controller disables the E-872 drive and the stage will not move. If the error is not null, then the closed-loop will act to control the system. In the same way, the stages 1, 2, 3 and 4 were associated with, respectively, virtual motors 31, 32, 33 and 34.

VALIDATION TESTS

Dead Band

This section shows the results of the embedded implementations explained in this paper, in terms of dead band and code architecture. Figure 6 shows an acquisition of approximately 2 minutes in the Motors 31, 32 and 33 – remembering they represent the stages of the vertical focusing mirror, and each m.u. (or motor unit) represents 1 nm –, and

ISBN: 978-3-95450-238-7 ISSN: 2226-0358 doi:10.18429/JACoW-ICALEPCS2023-TUMBCM034

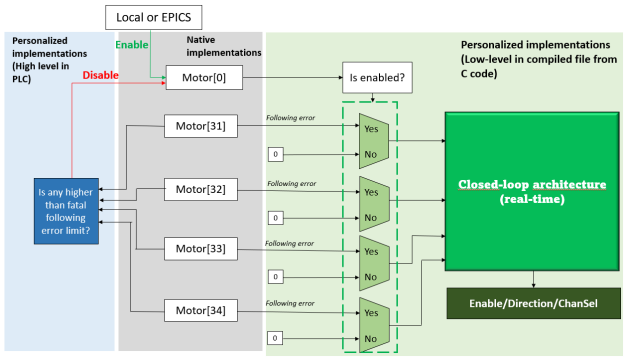

Figure 5: Scheme showing the mix of native and personalized implementations, aiming to improve the system safety.

it is evident that the oscillations are kept inside the mentioned dead band of 1 nm.

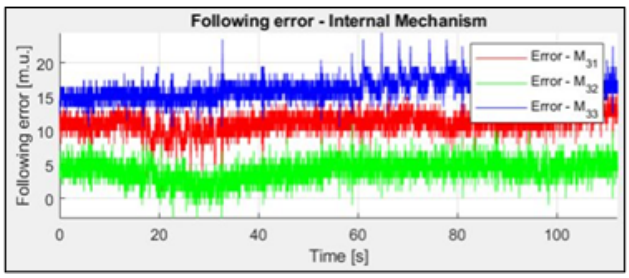

Figure 6: Vertical focusing mirror: following error acquisition for approximately 2 minutes.

As mentioned in [3], each step provided by the sawtooth wave delivered by the E-872 driver brings a movement of approximately 20 nm in the encoder attached next to the stage, in both horizontal and vertical focusing mirrors. So the dead band of 30 nm is acceptable for this project. This acquisition has also demonstrated the repeatability and nano precision of the construction with three piezoelectric stages arranged in a tripod.

Kinematics by Steps

This section shows the results of the embedded implementations explained in this paper, in terms of control and kinematics by steps a safety movement. To demonstrate the effectiveness of the closed loop for the horizontal focusing mirror – this one does not need a kinematics by steps for extra safety, as it is a 1-to-1 system — a simple movement is shown in the Fig. 7 – in which each unit represents 1 nm in the encoder scale. It is possible to realize the movement is stable from one point to the other.

To demonstrate the effectiveness of the kinematics by steps procedure, a simple movement in the vertical focusing mirror is shown in the Fig. 8. The range shown in this example is not enough to travel from one stripe to the other – it takes several minutes to complete, as the switching frequency of the E-872 driver is away from its maximum value (2.5 kHz) in order to accomplish with the closed-loop rate inside the PBLV controller.

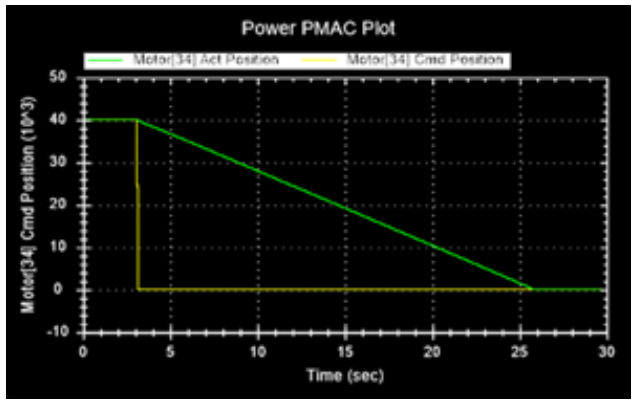

Figure 7: Simple stable movement in the horizontal focusing mirror.

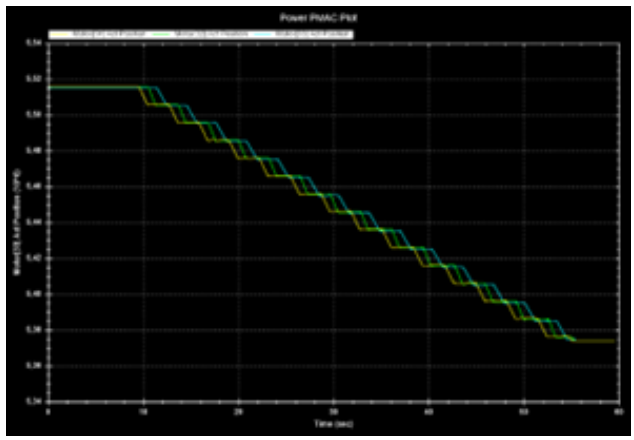

Figure 8: Example of kinematics by steps in the vertical focusing mirror.

CONCLUSION

A motion control architecture based on a low-level communication between a PBLV controller and a E-872 driver, in addition to a set of piezoelectric stages and encoders, has brought stability and functionalities that match the beamline expectations and requirements. The mechatronic design guarantees the beam stability without losing alignment flexibility and the adjustment can be done quickly by the experimental team staff. The nano-resolution, together with the designed controller system, also guarantees repeatability in the motion, which includes both internal mechanism and the long-stroke, represented by the granite bench.

ACKNOWLEDGEMENTS

The authors would like to gratefully acknowledge the funding by the Brazilian Ministry of Science, Technology, Innovation and the contribution of the LNLS team – other support groups responsible by the mechatronic design of the internal mechanism, installations assembly, electric infrastructure, automation, project management and the MOGNO Beamline staff.

ISBN: 978-3-95450-238-7 ISSN: 2226-0358 doi:10.18429/JACoW-ICALEPCS2023-TUMBCM034

REFERENCES

[1] N. L. Archilha *et al.*, "MOGNO, the nano and microtomography beamline at Sirius, the Brazilian synchrotron light source", *J. Phys. Conf. Ser.*, vol. 2380, p. 012123, 2022. doi:10.1088/1742-6596/2380/1/012123

[2] Sirius: accelerating the future of Brazilian science, https://www.lnls.cnpem.br/sirius-en/

[3] G. B. Z. L. Moreno *et al.*, "Multi-axis exactly-constrained mirror stages with Peltier cooling for high-flux hard X-ray nanofocusing", presented at European Society for Precision Engineering and Nanotechnology, 23rd International Conference, Copenhagen, Denmark, 2023.

[4] R. R. Geraldes *et al.*, "Granite Benches for Sirius X-ray Optical Systems", in *Proc. MEDSI'18*, Paris, France, Jun. 2018, pp. 361–364. doi:10.18429/JACoW-MEDSI2018-THPH12

[5] G. N. Kontogiorgos, A. Y. Horita, L. Martins dos Santos, M. A. L. Moraes, and L. F. Segalla, "The Mirror Systems Benches Kinematics Development for Sirius/LNLS", in *Proc. ICALEPCS'21*, Shanghai, China, Oct. 2021, pp. 358–361. doi:10.18429/JACoW-ICALEPCS2021-TUPV001

[6] J. P. Merlet, *Parallel Robots*. Springer-Verlag GmbH, July 2006. doi:10.1007/1-4020-4133-0

[7] Physik Instrumente (PI) GmbH & Co. KG, https://www.physikinstrumente.com/en/

[8] Renishaw plc, https://www.renishaw.com/en/

[9] J. J. Craig, *Introduction to Robotics: mechanics and control*. Upper Saddle River: Pearson Education International, 2005.

[10] J.C. Ehiwario and S.O. Aghamie, "Comparative study of bisection, Newton-Raphson and secant methods of root finding problems", *IOSR J. Eng.*, vol. 4, no. 4, pp. 01–07, 2014. doi:10.9790/3021-04410107

[11] Thomas Kluyver *et al.*, "Jupyter notebooks - a publishing format for reproducible computational workflows", in *Proc. 20th Int. Conf. Electronn. Publ.*, 2016, pp. 87–90. doi:10.3233/978-1-61499-649-1-87

[12] F. Milano and G. M. Jonsdottir, "Jupyter notebooks for computer-based laboratories on power system dynamics and control", in *10th Int. Conf. Educ. New Learn. Technol.*, 2018, pp. 112–121. doi:10.21125/edulearn.2018.0044

[13] Power PMAC User's Manual, https://assets.omron.com/m/2c1a63d391d6bfa3/